

Retournement temporel et quantification : quel équilibre entre module et phase pour la transmission d'énergie sans fil ?

Thomas CHOVÉ Yanis MERAKEB Julien HUILLERY

Univ Lyon, Ecole Centrale de Lyon, INSA Lyon, Université Claude Bernard Lyon 1, CNRS, Ampère, UMR5005
69130 Ecully, France

Résumé – Les performances du retournement temporel pour la transmission d'énergie sans fil à travers un milieu de propagation complexe sont étudiées sous une contrainte de quantification des signaux émis. Différentes méthodes de quantification sont utilisées afin de déterminer comment la précision de quantification doit être répartie entre le module et la phase des signaux définis en bande de base. À l'aide de simulations numériques, il est montré qu'un nombre égal de bits doit être alloué au module et à la phase lorsque la quantification est effectuée dans le domaine temporel et qu'un nombre plus important de bits doivent être alloués à la phase lorsque la quantification est effectuée dans le domaine fréquentiel.

Abstract – The performance of quantized time reversal for wireless power transfer through complex propagation medium are studied. Different quantization methods are used in order to determine how quantization precision should be distributed between the modulus and the phase of the emitted baseband signals. Using numerical simulations, it is shown that a similar number of bits must be allocated to the modulus and the phase when quantization is performed in the time domain and that more bits must be allocated to the phase for frequency-domain quantization.

1 Introduction

Time Reversal (TR) processing, which allows one to focus signals both spatially and temporally, was first used with acoustic waves [4], before being extended to electromagnetic waves [8]. It consists in taking into account the multipath or dispersive effects of propagation in the design of the emitted waveform in order to obtain a high peak power at the receiver. With Radio-Frequency (RF) waves, this technique was shown to allow better performance in complex multipath environments for information transmission [6] and, more recently, for Wireless Power Transfer (WPT) [11].

However, TR processing requires the use of precise complex waveforms, and is quite a sensitive technique. Furthermore, due to the digital nature of the systems used for RF applications, all stored and processed information is quantized. It is then necessary to know how quantization deteriorates the performance of TR processing. This question has already been addressed from the physicist point of view, studying the focusing properties of the waves [7, 10], as well as from the communication point of view where the performance is assessed through channel capacity or bit error rate [1, 2, 5]. Most of these studies are based on real-valued channel impulse response (CIR) models and signals [5, 10] or are dedicated to one-bit quantization [1, 2, 7].

In this paper, the approach is slightly different: first, the performance of quantized TR is studied in the context of WPT. This means that it is necessary to create a high peak power at the receiver location [3], but that the signal-to-noise ratio (SNR) needs not be optimised. Second, the question asked is that of the relative importance of the modulus and phase of the baseband signal to be emitted: it is sought to determine which of the modulus and phase should be coded with the highest precision to optimise WPT. The answer to this question will provide insights about the channel characteristics

that are the most relevant to WPT and a guideline for optimal RF waveforms design. To address these questions, a general quantization scheme allowing a given number of bits to be distributed arbitrarily between the modulus and the phase of a baseband signal is introduced. Using a WPT-specific performance criterion, numerical simulations based on a Rayleigh channel model are then carried out to compare the performance of several modulus/phase quantization strategies.

The rest of the paper is organized as follows: section 2 presents the system model and the WPT performance criteria used to compare the different quantization schemes. In section 3, modulus/phase quantization schemes are introduced. Section 4 describes the simulation set-up and results allowing determining the relative importance of modulus and phase. Finally, section 5 gives the conclusions of this work.¹

2 Signal model and evaluation criterion

2.1 Time reversal processing

We consider an emitted signal $x(t)$ passing through a channel whose CIR is denoted $h(t)$, giving a received signal $z(t) = x \star h(t)$, \star being the convolution product. The CIR is assumed to be perfectly known, at least within a frequency band of width B centred around a carrier frequency ν_c . It is assumed that modulation at the carrier frequency ν_c occurs after the design of the emitted signal, therefore all signals will be considered in baseband $[-B/2; B/2]$ and will be complex valued.

TR processing intends to design an emitted signal $x(t)$ such that the signal $z(t)$ received after propagation through the channel admits a maximum peak power at a given focusing

¹. Ce travail a bénéficié du soutien de la région Auvergne-Rhône-Alpes à travers le projet AMiTEIC n°19 009957 01 - 38866.

time T_0 . It solves the following problem:

$$\begin{cases} \max_x |z(T_0)|^2 = \left| \int_{-\infty}^{+\infty} h(t)x^*(T_0 - t)dt \right|^2 \\ \text{s.t. } \frac{1}{T_0} \int_0^{T_0} |x(t)|^2 dt \leq P_0 \end{cases} \quad (1)$$

Given the Cauchy-Schwartz inequality, the received peak power $|z(T_0)|^2$ is maximal for $x(t) = h^*(T_0 - t)$, where $*$ denotes complex conjugate. In practice, it is necessary to limit the spectrum of the emitted signal to the frequency band of interest $[-B/2; B/2]$ as well as its duration in time to T_w . To that aim, a sinc-hann pulse $w(t)$ defined as

$$w(t) = \text{sinc}(Bt) \text{hann}(t/T_w) \quad (2)$$

where $\text{hann}(t)$ denotes the Hanning window defined for $t \in [-1/2; 1/2]$, can be used such that the ideal TR emitted signal is given by

$$x_{\text{ideal}}(t) = h^*(T_0 - t) \star w(t). \quad (3)$$

The signal $z_{\text{ideal}}(t)$ received is therefore given by

$$z_{\text{ideal}}(t) = h \star x_{\text{ideal}}(t) = \mathcal{R}_h(t - T_0) \star w(t), \quad (4)$$

$\mathcal{R}_h(t)$ being the autocorrelation function of the CIR, leading $|z_{\text{ideal}}(t)|^2$ to be maximum for $t = T_0$. In the frequency domain, the Fourier transform of the emitted signal is given by

$$\begin{aligned} X_{\text{ideal}}(\nu) &= e^{-2i\pi\nu T_0} H^*(\nu)W(\nu) \\ &= e^{-2i\pi\nu T_0} |H(\nu)|e^{-i\varphi(\nu)}W(\nu) \end{aligned} \quad (5)$$

with $W(\nu)$ and $H(\nu) = |H(\nu)|e^{i\varphi(\nu)}$ the Fourier transform of $w(t)$ and $h(t)$ respectively. Accordingly, the Fourier transform of the signal received in this ideal situation is given by

$$Z_{\text{ideal}}(\nu) = e^{-2i\pi\nu T_0} |H(\nu)|^2 W(\nu). \quad (6)$$

These frequency-domain expressions highlight the two components involved in TR processing: the modulus of X_{ideal} is such that the emitted power is distributed according to the transmission capabilities of the channel; the phase of X_{ideal} is such that all frequency components arrive constructively at $t = T_0$ after propagation through the channel.

2.2 WPT Performance criterion

Several performance criteria can be used to evaluate the performance of WPT systems. These criteria generally describe the quantity of energy that is transferred from the source to the receiver, and how it is focused in time and/or space. Among them, the Peak-to-Emitted Power Ratio (PEPR) defined as

$$PEPR = \frac{|z(T_0)|^2}{\frac{1}{T_0} \int_0^{T_0} |x(t)|^2 dt}. \quad (7)$$

is the one used in this study. The PEPR evaluates the ratio of the peak power obtained at the receiver at a given time T_0 to the average power emitted by the source. It is an essential criterion for WPT systems as it determines the performance of the RF-DC rectifier circuits used at the receiver to collect the power [3]. Note that TR processing being based on PEPR maximization (see (1)), one may not expect higher PEPRs with quantized TR signals than without quantization.

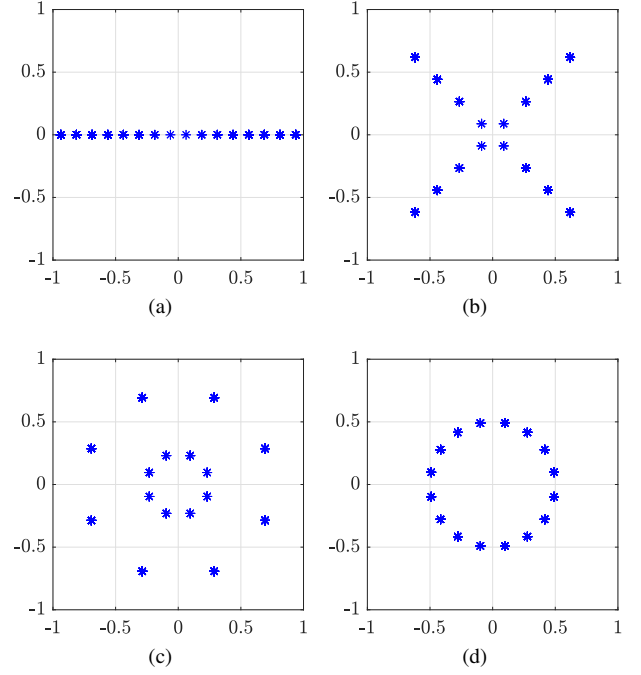


Figure 1 – MP quantization schemes for $N_{\text{bits}} = 4$: (a) $\Sigma(3, 1)$; (b) $\Sigma(2, 2)$; (c) $\Sigma(1, 3)$; (d) $\Sigma(0, 4)$

3 Modulus/phase quantization schemes

A family of Modulus/Phase (MP) quantization schemes is introduced in this section, allowing to arbitrarily distribute the quantization accuracy between the modulus and the phase of a complex-valued signal. Given a number of bits N_{bits} , an MP quantization scheme is denoted $\Sigma(N_m, N_\varphi)$, with $N_m + N_\varphi = N_{\text{bits}}$, where N_m is the number of bits used to uniformly quantize the modulus on $[0, 1]$ and N_φ is the number of bits used to uniformly quantize the phase on $[0, 2\pi]$. Considering a complex-valued signal $s(t) = |s(t)|e^{i\varphi(s(t))}$ with $|s(t)| \leq 1$, the quantized signal $\tilde{s}(t)$ is obtained by

$$\begin{aligned} \tilde{s}(t) &= \mathbf{Q}_{(N_m, N_\varphi)}[s(t)] \\ &= \mathbf{Q}_{N_m}^{[0, 1]}[|s(t)|] e^{i\mathbf{Q}_{N_\varphi}^{[0, 2\pi]}[\varphi(s(t))]} \end{aligned} \quad (8)$$

where $\mathbf{Q}_N^I[\bullet]$ denotes uniform quantization with N bits on the interval I . Note that phase and modulus quantizations are, with this method, decoupled. Figure 1 gives examples of MP quantization schemes obtained for $N_{\text{bits}} = 4$, from $\Sigma(3, 1)$ to $\Sigma(0, 4)$. One may note that $\Sigma(0, N_{\text{bits}})$ is equivalent to a PSK constellation diagram and quantizes only the phase of the signal, while $\Sigma(N_{\text{bits}} - 1, 1)$ is equivalent to an ASK constellation diagram and quantizes only the amplitude of the real part of the signal.

The MP quantization schemes above will be applied with two dual approaches, namely time-domain quantization and frequency-domain quantization. For time-domain quantization, the emitted signal $\tilde{x}(t)$ is the quantized version of the ideal TR waveform $x_{\text{ideal}}(t)$ defined in (3), hence

$$\tilde{x}(t) = \mathbf{Q}_{(N_m, N_\varphi)}[x_{\text{ideal}}(t)] \quad (9)$$

For frequency-domain quantization, the spectrum of the emitted signal is the quantized version of the ideal TR waveform

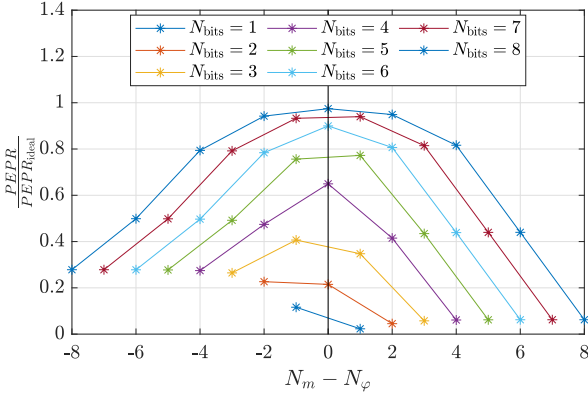


Figure 2 – Mean PEPR as a function of N_{bits} and for all MP quantization schemes $\Sigma(N_m, N_\varphi)$ for time-domain quantization. (see color online)

spectrum $X_{\text{ideal}}(\nu)$ defined in (5), hence

$$\tilde{X}(\nu) = \mathbf{Q}_{(N_m, N_\varphi)}[X_{\text{ideal}}(\nu)] \quad (10)$$

Note that quantizing in the frequency domain may probably not be adapted to usual emitters. However, comparing the two approaches will reveal the relative importance of the information carried by the modulus and phase in the time and the frequency domains. It also gives some clues regarding the storage of the CIR in the time or frequency domain.

4 Simulation results

4.1 Propagation channel model and simulation set-up

The channel model used in this study is a generic Rayleigh channel model, the CIR of which is given by

$$\forall t \in [0; T_0], h(t) = a(t)e^{-\tau t}, \quad (11)$$

with $a(t)$ a complex circular Gaussian iid random process. In the sequel, the CIR duration is $T_0 = 400$ ns, the exponential decay rate is $\tau = 30$ ns and the variance of both the real and imaginary parts of $a(t)$ is normalized such that the mean spectral power is 10^{-3} . Those parameters have been chosen to mimic the real-life experimental RF platform reported in [9]. Finally, 1000 realizations of the CIR were generated for each quantization configuration and the results presented hereafter are the mean performance over these 1000 realizations.

4.2 Optimal balance between modulus and phase

For a given number of bits N_{bits} ranging from 1 to 8, the mean PEPR (normalized by the one obtained with ideal signals) obtained with the MP quantization schemes ranging from $\Sigma(0, N_{\text{bits}})$ to $\Sigma(N_{\text{bits}}, 0)$ is presented in figure 2 for time-domain quantization and figure 3 for frequency-domain quantization. The quantization schemes on the right of the figures are those allocating more precision to the modulus ($N_m > N_\varphi$) while those on the left allocate more precision to the phase ($N_\varphi > N_m$).

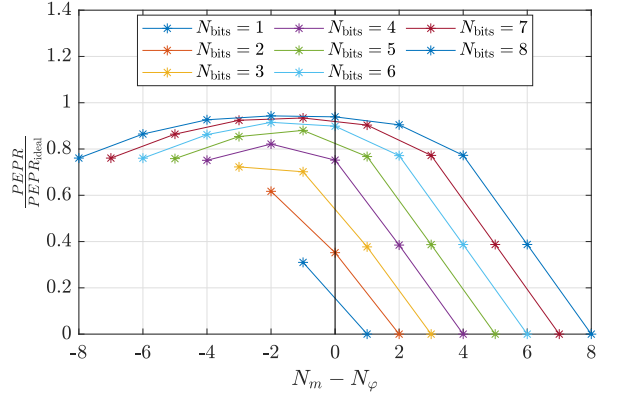


Figure 3 – Mean PEPR as a function of N_{bits} and for all MP quantization schemes $\Sigma(N_m, N_\varphi)$ for frequency-domain quantization. (see color online)

For time-domain quantization (figure 2), it is observed that modulus and phase are somehow equally important. When N_{bits} is an even number, the optimal balance (given by the position of the maximum of the curves) is $N_m = N_\varphi$, except for $N_{\text{bits}} = 2$ for which the phase must be favoured. When N_{bits} is an odd number, the optimal balance is $N_m = N_\varphi - 1$ when $N_{\text{bits}} \leq 3$ (allocate one more bit to the phase) and $N_m = N_\varphi \pm 1$ (arbitrarily allocate one more bit to the phase or to the modulus) when $N_{\text{bits}} \geq 5$. For frequency-domain quantization (figure 3), it is however clearly observed that the best quantization strategy is to allocate one or two more bits to the phase than to the modulus (the maximum of the curves always lies on the left side of the graph). This means that the information carried by the phase of the frequency response of the channel (making components interfere constructively) is more important for WPT than the information carried by the modulus. Interestingly, it is to be noted that when $N_{\text{bits}} \leq 6$, frequency-domain quantization provides better WPT performance than time-domain quantization.

4.3 Comparison with classical constellation diagrams

In this subsection, the performance of quantization schemes directly inspired from classical digital communication constellation diagrams, namely the PSK, ASK and QAM, is studied and compared with the previously proposed optimally balanced MP quantization schemes. The PSK and ASK constellation diagrams symbolize the two extreme cases of phase-only and amplitude-only quantization. As noted earlier, they are special cases of MP quantization schemes. The QAM quantization scheme allocates an equal number of bits to the real and imaginary parts of the signal. It is worth noting that in this process, QAM codes the phase with more precision than the modulus (e.g., the 16-QAM allows 12 phase values and 3 modulus values).

The figure 4 (resp. 5) presents the mean PEPR as a function of N_{bits} obtained for time-domain (resp. frequency-domain) quantization with (i) the optimally balanced MP quantization scheme (blue stars), denoted OBMP hereafter, the optimal couple (N_m, N_φ) being indicated for each value of N_{bits} , (ii) the QAM constellation diagram (yellow circles), (iii) the PSK constellation diagram (red crosses) and (iv) the signed ASK

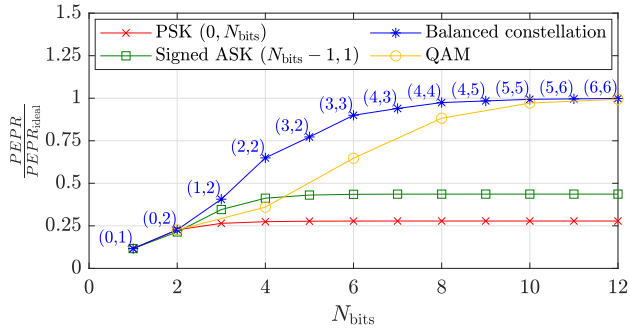


Figure 4 – Mean PEPR as a function of N_{bits} for time-domain quantization. For each point, the (N_m, N_φ) couple of the optimally balanced MP quantization scheme is given.

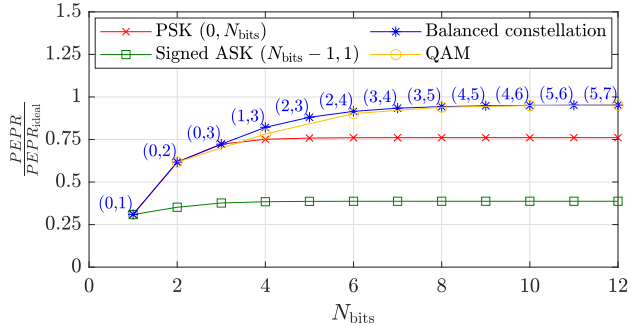


Figure 5 – Mean PEPR as a function of N_{bits} for frequency-domain quantization. For each point, the (N_m, N_φ) couple of the optimally balanced MP quantization scheme is given.

constellation diagram (green squares). For time-domain quantization, QAM and OBMP quantization schemes reach the optimal performance as N_{bits} increases. However, for intermediary numbers of bits ($N_{\text{bits}} < 10$), the QAM performance are lower than those obtained with OBMP: QAM quantization allocates too much precision to the phase, neglecting the somehow equal importance of the modulus. For frequency-domain quantization, QAM and OBPM quantization schemes have similar performance for any value of N_{bits} . This is related to the fact that optimal frequency-domain quantization requires allocating more precision to the phase than to the modulus, which is the natural behaviour of QAM constellations..

5 Conclusion

In this paper, the optimal way to allocate quantization precision between the modulus and the phase of baseband signal was investigated in the context of TR processing for WPT. In order to do this, MP quantization schemes were introduced, authorizing an arbitrary allocation of quantization bits over modulus and phase and numerical simulations with a Rayleigh channel model was conducted. According to the PEPR performance criterion, it was shown that the optimal balance is obtained by allocating a similar number of bits to the phase and to the modulus when quantization is performed in the time domain, while more bits must be allocated to the phase when quantization is performed in the frequency domain. Also, as compared to classical digital communication constellation diagrams like QAM, the optimally balanced MP quantization scheme demonstrates a clear improvement for intermediary

number of bits (from 3 to 8). Finally, it was shown that for a budget greater that $N_{\text{min}} = 8$ bits, the impact of quantization on WPT becomes negligible. Those results provide a guideline to the optimal waveform design problem in the context of WPT as soon as quantization constraints must be taken into account.

References

- [1] Dariush Abbasi-Moghadam and Vahid Tabataba Vakili. A SIMO one-bit time reversal for UWB communication systems. *EURASIP Journal on Wireless Communications and Networking*, 2012(1):113, March 2012.
- [2] Yu-Hao Chang, Shang-Ho Tsai, Xiaoli Yu, and C.-C. Jay Kuo. Ultrawideband Transceiver Design Using Channel Phase Precoding. *IEEE Transactions on Signal Processing*, 55(7):3807–3822, July 2007.
- [3] A. Collado and A. Georgiadis. Optimal Waveforms for Efficient Wireless Power Transmission. *IEEE Microwave and Wireless Components Letters*, 24(5):354–356, May 2014.
- [4] M. Fink, C. Prada, F. Wu, and D. Cassereau. Self focusing in inhomogeneous media with time reversal acoustic mirrors. In *Proceedings., IEEE Ultrasonics Symposium*, pages 681–686 vol.2, October 1989.
- [5] Yi Han, Yan Chen, and K. J. Ray Liu. Time-reversal with limited signature precision: Tradeoff between complexity and performance. In *2014 IEEE Global Conference on Signal and Information Processing (GlobalSIP)*, pages 664–668, December 2014.
- [6] Yi Han, Yan Chen, Beibei Wang, and K. J. Ray Liu. Time-Reversal Massive Multipath Effect: A Single-Antenna “Massive MIMO” Solution. *IEEE Transactions on Communications*, 64(8):3382–3394, August 2016.
- [7] Kyritsi and Papanicolaou. One-bit Time Reversal for WLAN Applications. In *2005 IEEE 16th International Symposium on Personal, Indoor and Mobile Radio Communications*, volume 1, pages 532–536, 2005.
- [8] G. Lerosey, J. de Rosny, A. Tourin, A. Derode, G. Montaldo, and M. Fink. Time Reversal of Electromagnetic Waves. *Phys. Rev. Lett.*, 92(19):193904, May 2004. Publisher: American Physical Society.
- [9] Yanis Merakeb, Hussein Ezzeddine, Julien Huillery, Arnaud Bréard, Rachida Touhami, and Yvan Duroc. Experimental demonstration of a passive UHF RFID communication in time reversal and pulsed wave mode. In *2019 IEEE International Conference on RFID Technology and Applications (RFID-TA)*, pages 58–62, 2019.
- [10] P. Sundaralingam and V. Fusco. Effect of quantisation and under sampling on time reversal spatial and temporal focussing in highly reverberant environment. In *2011 41st European Microwave Conference*, pages 416–419, October 2011.
- [11] Mohammad R. Vedady Moghadam, Yong Zeng, and Rui Zhang. Waveform optimization for radio-frequency wireless power transfer. In *IEEE 18th International Workshop on Signal Processing Advances in Wireless Communications (SPAWC)*, pages 1–6, July 2017. ISSN: 1948-3252.